A Circuit Model of a System of VLSI Interconnects for Time Response Computation

Rui Wang, *Member, IEEE*, and Omar Wing, *Fellow, IEEE*

***Abstract*—A new computational model based on the spectral-domain approach for the characterization of a dispersive multiconductor system is developed for time response computation. The model consists of two identical impedance networks and equivalent voltage-controlled voltage sources and it is particularly suitable for timing analysis. Since full-wave analysis is employed for the derivation, the computational model is valid at very high frequencies when the longitudinal field components are no longer negligible.**

I. Introduction

NUMERICAL characterization and modeling of multiconductor transmission line systems have been the subject of extensive study for many years. Among the methods commonly employed, the most preferred and prominently used is the spectral–domain approach (SDA), which was first applied to the computation of slotline dispersion characteristics [1] and microstrip characteristics [2] by Itoh and Mittra. Numerous publications followed with a variety of fundamental applications and modifications [3]. However, few have utilized the results obtained from these full-wave analyses to develop suitable computational models for transient analysis of VLSI interconnects terminated in nonlinear circuits. Most transient analyses are still based on the static per-unit-length parameters of the multiconductor systems. Such a characterization is geared toward TEM approximation, and the accuracy of the approximation decreases with increasing frequencies. In this paper, we introduce a new computational model based on full-wave analysis which takes into account all possible field components and satisfies all the required boundary conditions in the structure to characterize a dispersive multiconductor system. Moreover, the model is particularly suitable for circuit simulation.

II. Scattering Matrix of a Multiconductor System

We are given a multiconductor microstrip system embedded in an inhomogeneous dielectric medium as shown in Fig. 1. The system is enclosed in a conductor box of width $2a$ and height $h_1+h_2+h_3+h_4$. Following an approach similar to that taken by Jansen [4], we first expand the electromagnetic fields into longitudinal-section electric (LSE) and longitudinal-section magnetic (LSM) fields. Let $\Phi(x,y)$ and $\Psi(x,y)$ be the scalar potentials corresponding to LSE and LSM fields respectively. They can be written, for each dielectric region shown in Fig. 1, as

$$\Phi_1=\sum_n A_n \operatorname{Si}(k_{xn}x)\sin\left[k_{yn1}(y+h_1+h_2)\right]$$

$$\Psi_1=\sum_n B_n \operatorname{Ci}(k_{xn}x)\cos\left[k_{yn1}(y+h_1+h_2)\right]$$

$$\Phi_2=\sum_n \{C_n\sin\left[k_{yn2}(y+h_2)\right] + D_n\cos\left[k_{yn2}(y+h_2)\right]\}\operatorname{Si}(k_{xn}x)$$

$$\Psi_2=\sum_n \{E_n\sin\left[k_{yn2}(y+h_2)\right] + F_n\cos\left[k_{yn2}(y+h_2)\right]\}\operatorname{Ci}(k_{xn}x)$$

$$\Phi_3=\sum_n \{G_n\sin\left[k_{yn3}(y-h_3)\right] + H_n\cos\left[k_{yn3}(y-h_3)\right]\}\operatorname{Si}(k_{xn}x)$$

$$\Psi_3=\sum_n \{I_n\sin\left[k_{yn3}(y-h_3)\right] + L_n\cos\left[k_{yn3}(y-h_3)\right]\}\operatorname{Ci}(k_{xn}x)$$

$$\Phi_4=\sum_n O_n \operatorname{Si}(k_{xn}x)\sin\left[k_{yn4}(y-h_3-h_4)\right]$$

$$\Psi_4=\sum_n P_n \operatorname{Ci}(k_{xn}x)\cos\left[k_{yn4}(y-h_3-h_4)\right] \qquad (1)$$

Manuscript received June 12, 1990; revised December 10, 1990. This work was supported by the National Science foundation under Grant NSF ECD 88-11111 and by the New York State Center for Advanced Technology—Computer and Information Systems.

R. Wang was with the Department of Electrical Engineering, Columbia University, New York, NY 10027. She is now with Cadence Design Systems, Santa Clara, CA 95054.

O. Wing is with the Department of Electrical Engineering, Columbia University, New York, NY 10027.

IEEE Log Number 9042494.

0018-9480/91/0400-0688$01.00 ©1991 IEEE

where

$$\mathrm{Si}(x)=\begin{cases}\sin(x)\\ \cos(x)\end{cases}$$

$$\mathrm{Ci}(x)=\begin{cases}\cos(x)\\ \sin(x)\end{cases} \tag{2}$$

$$k_{xn}=\begin{cases}(2n-1)\pi/2a\\ (n-1)\pi/a\end{cases} \tag{3}$$

and

$$k_{yni}=\sqrt{\omega^2\epsilon_i\mu+\gamma^2-k_{xn}^2}. \tag{4}$$

In (2)–(4), the upper terms refer to the even modes (magnetic wall in the plane of symmetry $x=0$) and the lower terms to the odd modes (electric wall at $x=0$). Notice that the boundary conditions at $x=\pm a$, $y=h_3+h_4$, and $y=-h_1-h_2$ are automatically satisfied.

By matching the boundary conditions to eliminate all unknown coefficients in (1), we find a set of algebraic equations relating the spectral-domain electric fields to the current distribution:

$$\begin{bmatrix}E_{xn}(k_{xn})\\ E_{zn}(k_{xn})\end{bmatrix}=\begin{bmatrix}Z_{xxn} & Z_{xzn}\\ Z_{zxn} & Z_{zzn}\end{bmatrix}\begin{bmatrix}J_{xn}(k_{xn})\\ J_{zn}(k_{xn})\end{bmatrix}. \tag{5}$$

Here Z_{xxn}, etc., are spectral-domain Green's functions. With proper normalization, they can be made real functions for lossless dielectric media and complex for lossy media.

The unknown current distribution functions J_{xn} and J_{zn} are expanded in terms of known basis functions J_{xn}^{pq} and J_{zn}^{pq}:

$$J_{xn}=\sum_{p=1}^{N}\sum_{q=1}^{M}c_{pq}J_{xn}^{pq}(k_{xn})$$

$$J_{zn}=\sum_{p=1}^{N}\sum_{q=1}^{M}d_{pq}J_{zn}^{pq}(k_{xn}) \tag{6}$$

where c_{pq} and d_{pq} are unknown coefficients, N is the number of terms needed in the expansion, and M is the number of striplines in the system. The basis functions $J_{xn}^{pq}(k_{xn})$ and $J_{zn}^{pq}(k_{xn})$ are the spectral-domain counterparts of the spatial-domain basis functions $j_{xn}^{pq}(x)$ and $j_{zn}^{pq}(x)$, which must be chosen to approximate the true but unknown current distributions. Increasing the number of coefficients in (6) supplies an audit of the accuracy. It is obvious that we do not wish to have more basis elements than are strictly necessary because keeping N small, in consonance with accuracy, is a desirable objective. The basis functions chosen are

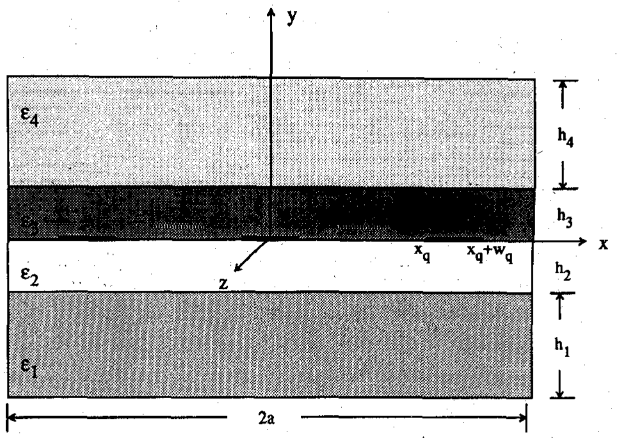

Fig. 1. Cross section of a typical multiconductor system.

By applying Galerkin's method in the spectral domain, a set of homogeneous equations can be derived:

$$[A(\gamma,\omega)][c]=0 \tag{9}$$

where $A(\gamma,\omega)$ is a $(2N\times M)\times(2N\times M)$ matrix, and $c=[c_{pq}d_{pq}]^P$, where $p=1\cdots N$ and $q=1\cdots M$, is a $2N\times M$ column vector which contains the unknown basis function coefficients.

In order to have nontrivial solutions of the unknown coefficients in (9), we must have

$$\det[A(\gamma,\omega)]=0. \tag{10}$$

Equation (10) is solved for the propagation constant γ for each frequency. The dispersion characteristics are thus computed. The first M roots found from (9), $\lceil M/2\rceil$ roots for the even mode and $\lfloor M/2\rfloor$ zeros for the odd mode, contribute to the M dominant modes in an M-line system. Throughout this paper, we assume that these are the only modal waves propagating.

Once the value of γ for each dominant mode is obtained, the solution for the coefficients can be found, up to a constant, by the least mean squares method. Without loss of generality, we set $c_{11}=1$, and the following equations are to be solved by singular value decomposition [9]:

$$\begin{bmatrix}A_{12} & A_{13} & \cdot & \cdot & A_{1,2NM}\\ A_{22} & A_{23} & \cdot & \cdot & A_{2,2NM}\\ \cdot & \cdot & \cdot & \cdot & \cdot\\ \cdot & \cdot & \cdot & \cdot & \cdot\\ \cdot & \cdot & \cdot & \cdot & \cdot\\ A_{2NM,2} & A_{2NM,3} & \cdot & \cdot & A_{2NM,2NM}\end{bmatrix}\begin{bmatrix}c_{12}\\ \cdot\\ c_{NM}\\ d_{11}\\ \cdot\\ d_{NM}\end{bmatrix}=-\begin{bmatrix}A_{11}\\ A_{21}\\ \cdot\\ \cdot\\ A_{2NM,1}\end{bmatrix}. \tag{11}$$

$$j_{xn}^{pq}=\begin{cases}\sin\left[p\pi\dfrac{2(x-x_q)}{w_q}\right]\left(1-\left[\dfrac{2(x-x_q)}{w_q}-1\right]^2\right)^{1/2}, & x_q<x<x_q+w_q\\ 0, & \text{elsewhere}\end{cases} \tag{7}$$

$$j_{zn}^{pq}=\begin{cases}\cos\left[p\pi\dfrac{2(x-x_q)}{w_q}\right]\Big/\left(1-\left[\dfrac{2(x-x_q)}{w_q}-1\right]^2\right)^{1/2}, & x_q<x<x_q+w_q\\ 0, & \text{elsewhere.}\end{cases} \tag{8}$$

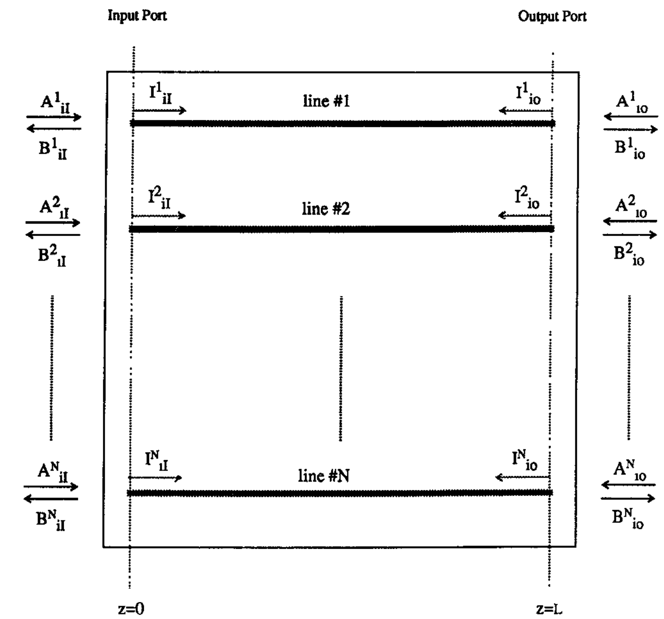

Fig. 2. N-conductor system with mode i excitation.

Now that the mode i propagation constant γ_i, and the coefficients c_{ij} and d_{ij}, $j=1,\cdots,N$, are known, we have a complete description for each propagating modal wave. In order to characterize these dominant modal waves, we define the relative current amplitudes on the striplines for each mode to be the *current eigen-amplitude vector* M_i:

$$M_i = [1 m_{2i} \cdots m_{Mi}]^T \tag{12}$$

in which m_{ki} denotes the mode i longitudinal current amplitude on line k normalized to the mode i current amplitude on line 1. The amplitude m_{ki} is computed by

$$m_{ki} = \frac{\sum_{j=1}^{N} \int_{x_k}^{x_k+w_k} d_{ij} j_{zn}^{ij}(x)\,dx}{\sum_{j=1}^{N} \int_{x_1}^{x_1+w_1} d_{ij} j_{zn}^{ij}(x)\,dx}. \tag{13}$$

Denote the mode i incident wave at the input port by $A_{iI} = [A_{iI}^1 A_{iI}^2 \cdots A_{iI}^N]^T$, in which A_{iI}^k represents the mode i incident wave amplitude on line k. The corresponding reflected wave at the input port is $B_{iI} = [B_{iI}^1 B_{iI}^2 \cdots B_{iI}^N]^T$. Similarly, A_{iO} and B_{iO} are the model incident and reflected wave amplitudes respectively, at the output port (see Fig. 2). By definition we have

$$A_{iI} = A_{iI}^1 M_i \qquad A_{iO} = A_{iO}^1 M_i$$
$$B_{iI} = B_{iI}^1 M_i \qquad B_{iO} = B_{iO}^1 M_i. \tag{14}$$

If the structure is infinitely long, we can write

$$\boldsymbol{B}_o = \begin{bmatrix} e^{-\gamma_1 L} & & \\ & \ddots & \\ & & e^{-\gamma_N L} \end{bmatrix} \boldsymbol{A}_I \tag{15a}$$

$$\boldsymbol{B}_I = \begin{bmatrix} e^{-\gamma_1 L} & & \\ & \ddots & \\ & & e^{-\gamma_N L} \end{bmatrix} \boldsymbol{A}_o \tag{15b}$$

in which

$$\boldsymbol{A}_o = [A_{1O}^1 A_{2O}^1 \cdots A_{NO}^1]^T$$

is the modal incident wave amplitude vector at the output port, and

$$\boldsymbol{B}_I = [B_{1I}^1 B_{2I}^1 \cdots B_{NI}^1]^T$$

is the modal reflected wave amplitude vector at the input port. The subscript I in the above denotes the input port, and O represents the output port. The modal scattering matrix of the wave structure is

$$\begin{bmatrix} \boldsymbol{B}_I \\ \boldsymbol{B}_o \end{bmatrix} = \begin{bmatrix} 0 & \operatorname{diag}(e^{\gamma_i L}) \\ \operatorname{diag}(e^{\gamma_i L}) & 0 \end{bmatrix} \begin{bmatrix} \boldsymbol{A}_I \\ \boldsymbol{A}_o \end{bmatrix}. \tag{16}$$

Now let us consider an arbitrary incident wave $a_I = [a_I^1 a_I^2 \cdots a_I^N]^T$ applied to the input port of the multiconductor system. This wave can be expressed as a linear combination of the dominant modal waves by the following equation:

$$a_I = A_{1I}^1 M_1 + A_{2I}^1 M_2 + \cdots + A_{NI}^1 M_N. \tag{17}$$

Define the modal eigenvector matrix M to be

$$M = [M_1 M_2 \cdots M_N]. \tag{18}$$

We have, in matrix form,

$$a_I = MA_I. \tag{19a}$$

The corresponding reflected wave at the input port b_I is given by

$$b_I = MB_I. \tag{19b}$$

For the output port, by the same token, we have

$$a_O = MA_O \tag{20a}$$

$$b_O = MB_O. \tag{20b}$$

Substitute (19) and (20) into (15):

$$\begin{bmatrix} b_I \\ b_O \end{bmatrix} = \begin{bmatrix} 0 & Me^{-\Gamma L}M^{-1} \\ Me^{-\Gamma L}M^{-1} & 0 \end{bmatrix} \begin{bmatrix} a_I \\ a_O \end{bmatrix} \tag{21}$$

where $e^{-\Gamma L} = \operatorname{diag}(e^{-\gamma_i L})$, $i = 1,2,\cdots,N$, is the modal propagation matrix. We have thus derived the scattering matrix of the N-conductor system. One should keep in mind that for a dispersive multiconductor system, both the propagation matrix $e^{-\Gamma L}$ and the eigenvector matrix M are frequency dependent. In general, off-diagonal terms in submatrix $Me^{-\Gamma L}M^{-1}$ are nonzero, accounting for the couplings between the lines.

III. Voltage-Based Computational Model

In order to compute the transient response of a multiconductor system terminated in linear and/or nonlinear loads, we need to find the relationship between the terminal voltages and currents of the system. Modal characteristic impedances are used to relate line voltages to line currents for a given mode. Unfortunately, because of the non-TEM nature of the multiconductor structure, the definition for the modal characteristic impedance is not unique. In this paper, we calculate characteristic impedances based on total power transported along the striplines. For a given dominant mode i, the complex power transported on an infinitely long line j is

$$P_{ij} = \iint (\boldsymbol{E}_{ij} \times \boldsymbol{H}_{ij}^*) \cdot \hat{z}\,dx\,dy = \iint (E_{xij} H_{yij}^* - E_{yij} H_{xij}^*)\,dx\,dy \tag{22}$$

where $\boldsymbol{E}_{ij}$ and $\boldsymbol{H}_{ij}$ are fields generated by the mode i current on line j. From the current–voltage description of the same system we have

$$P_{ij} = V_{ij} I_{ij}^* = Z_{ij} I_{ij} I_{ij}^*. \tag{23}$$

In the above equation, V_{ij} and I_{ij} are the mode i terminal voltage and current on line j. Combining (22) and (23), we get

$$Z_{ij} = \frac{\iint (\boldsymbol{E}_{ij} \times \boldsymbol{H}_{ij}^*) \cdot \hat{z}\, dz\, dy}{|I_{ij}|^2}. \tag{24}$$

The current I_{ij} can be calculated by a one-dimensional integration over the mode i longitudinal current distribution on line j.

Now let us proceed to define the terminal voltage and current vectors. If we relate the mode i input port terminal currents I_{iI} to the incident and reflected waves, i.e.,

$$I_{iI} = \begin{bmatrix} I_{iI}^1 \\ \vdots \\ I_{iI}^N \end{bmatrix} = \begin{bmatrix} A_{iI}^1 \\ \vdots \\ A_{iI}^N \end{bmatrix} - \begin{bmatrix} B_{iI}^1 \\ \vdots \\ B_{iI}^N \end{bmatrix} = (A_{iI}^1 - B_{iI}^1) \begin{bmatrix} m_{1i} \\ \vdots \\ m_{Ni} \end{bmatrix} \tag{25}$$

then the input port terminal voltages for mode i are given by

$$V_{iI} = \begin{bmatrix} V_{iI}^1 \\ \vdots \\ V_{iI}^N \end{bmatrix} = \begin{bmatrix} Z_{i1}(A_{iI}^1 + B_{iI}^1) \\ \vdots \\ Z_{iN}(A_{iI}^N + B_{iI}^N) \end{bmatrix} = (A_{iI}^1 + B_{iI}^1) \begin{bmatrix} Z_{1i} m_{1i} \\ \vdots \\ Z_{Ni} m_{Ni} \end{bmatrix}. \tag{26}$$

The total terminal currents and voltages at the input port are

$$I_I = \sum_{i=1}^{N} I_{iI} = M(A_I - B_I) = a_I - b_I \tag{27}$$

$$V_I = \sum_{i=1}^{N} V_{iI} = Z_m(A_I + B_I) = Z_m M^{-1}(a_I + b_I) \tag{28}$$

$$Z_m = \begin{bmatrix} m_{11} Z_{11} & \cdot & m_{1N} Z_{1N} \\ \cdot & \cdot & \cdot \\ m_{N1} Z_{N1} & \cdot & m_{NN} Z_{NN} \end{bmatrix}. \tag{29}$$

Similarly, for the output port

$$I_O = a_O - b_O \tag{30}$$

$$V_O = Z_m M^{-1}(a_O + b_O). \tag{31}$$

A system characteristic impedance matrix can be defined as

$$Z_c = Z_m M^{-1}. \tag{32}$$

Eliminating the wave terms (a_I, b_I, etc.) from the above, we have a description of the multiconductor system in terms of line voltages and currents:

$$V_I - Z_c I_I = Z_m e^{-\Gamma L} Z_m^{-1}(V_O + Z_c I_O) \tag{33a}$$

$$V_O - Z_c I_O = Z_m e^{-\Gamma L} Z_m^{-1}(V_I + Z_c I_I). \tag{33b}$$

It is immediately noticed that voltages and currents at the input port depend completely on the output voltages and currents, and vice versa. Let the voltage transmission matrix be

$$\Phi_U = Z_m e^{-\Gamma L} Z_m^{-1} \tag{34}$$

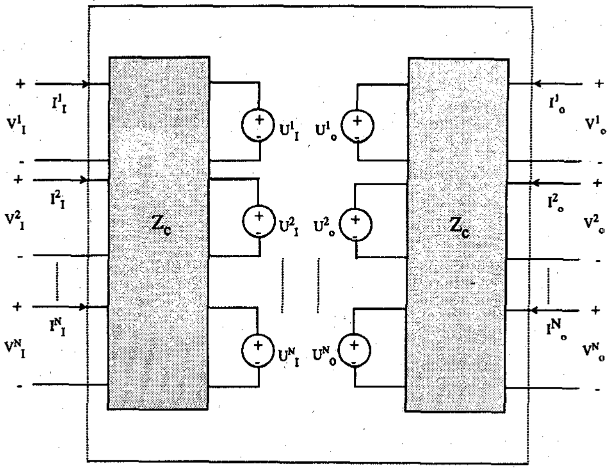

Fig. 3. Voltage-based computational model.

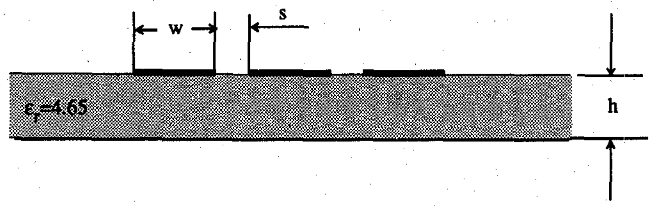

Fig. 4. A three-conductor structure: $w = h = 60$ mm, $s = 10$ mm, and $L = 30.48$ cm.

and define

$$U_I = \Phi_U(V_O + Z_c I_O) \tag{35a}$$

$$U_O = \Phi_U(V_I + Z_c I_I). \tag{35b}$$

Equations (33) then become

$$V_I = Z_c I_I + U_I \tag{36a}$$

$$V_O = Z_c I_O + U_O. \tag{36b}$$

Here U_I and U_O can be viewed as equivalent dependent voltage sources. After suitable manipulations, we eliminate the current terms and get

$$U_I = \Phi_U(2V_O - U_O) \tag{37a}$$

$$U_O = \Phi_U(2V_I - U_I). \tag{37b}$$

Equations (36) and (37), together with (34), represent our voltage-based frequency-domain computational model for the dispersive multiconductor system. The schematic model is shown in Fig. 3. It consists of two identical impedance networks Z_c combined with the voltage-controlled voltage sources U_I and U_O. It should be emphasized that the system is modeled completely in the frequency domain; thus all parameters characterizing the multiconductor systems can be frequency dependent. As pointed out earlier, the terminal voltages at one end of the multiconductor system are computed from the voltages at the other end. By defining the equivalent voltage sources, we can greatly simplify the transient analysis of such multiconductor systems terminated in nonlinear loads [7], [8].

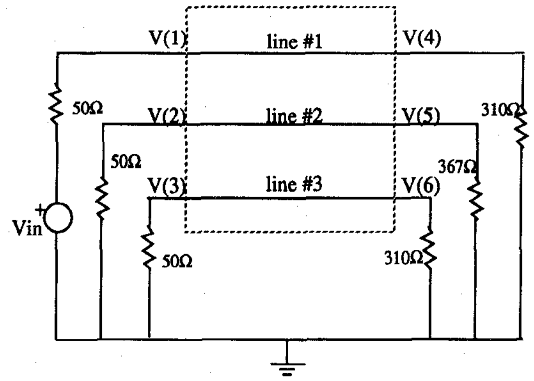

Fig. 5. Three-conductor system terminated in linear loads.

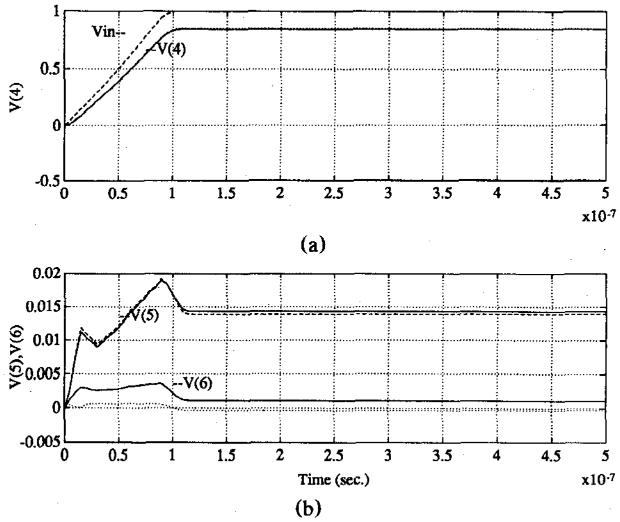

Fig. 6. TEM behavior of structure 5 at low frequencies.

IV. Signal Propagation Along a Multiconductor System Terminated in Linear Loads

The three-line microstrip structure shown in Fig. 4 is used to study pulse propagation along the lines. The purpose of this study is twofold. One, with a step excitation of slow rise time, we can verify the correctness of the full-wave models derived in this section by comparing results with those of the TEM model at low frequency. And, two, with a fast pulse input, we want to examine the non-TEM behavior at high frequency. The particular structure is chosen for the availability of both the TEM per-unit-length capacitance matrices and the physical stripline structure so that comparisons can be made. Lines are terminated with resistors at both input port and output port. A step excitation of 100 ns rise time is applied to line 1 (see Fig. 5). The per-unit-length capacitance matrices with and without the existence of the dielectric layer are [5]

$$C=\begin{bmatrix} 1.0413 & -0.3432 & -0.0140 \\ -0.3432 & 1.1987 & -0.3432 \\ -0.0140 & -0.3432 & 1.0413 \end{bmatrix} \text{pF/cm} \quad (38)$$

$$\overline{C}=\begin{bmatrix} 0.3516 & -0.1482 & -0.0127 \\ -0.1482 & 0.4293 & -0.1482 \\ -0.0127 & -0.1482 & 0.3516 \end{bmatrix} \text{pF/cm.} \quad (39)$$

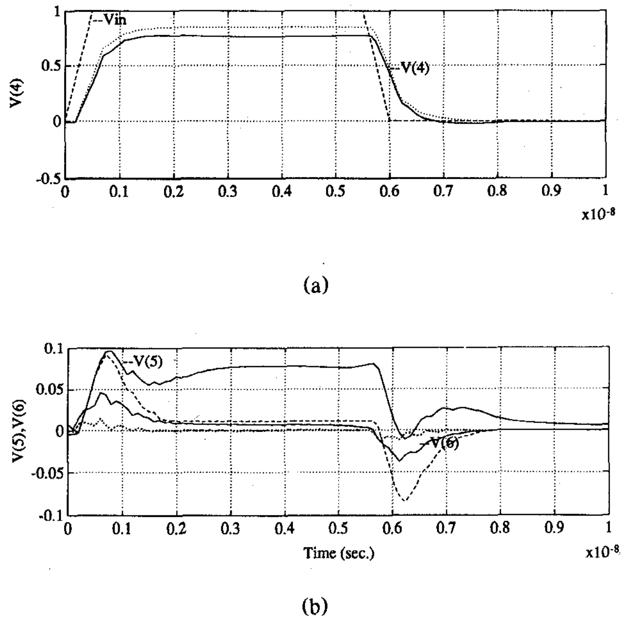

Fig. 7. Non-TEM behavior of structure 5 at high frequencies.

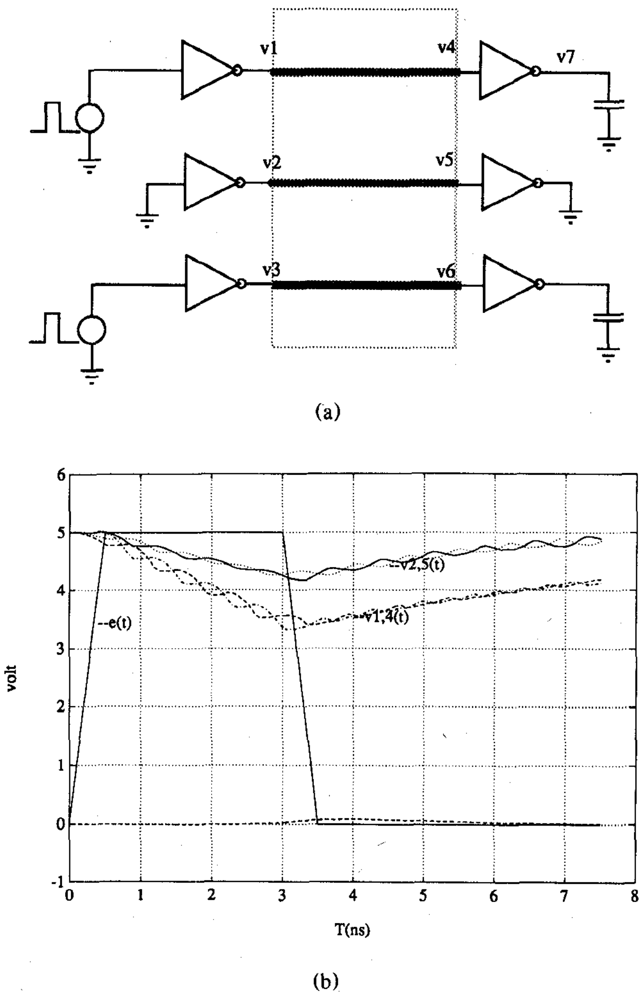

Fig. 8. (a) Three-conductor system terminated in CMOS inverters. (b) Voltage response of circuit in Fig. 8(a).

Since terminations are linear, the responding waveforms can be calculated in the frequency domain and then transformed to the time domain by the Fourier transform. The output signals computed by using our model and the TEM model in [5] are plotted in Fig. 6. One can see the nearly identical results, as expected. Notice that a closed structure is used to approximate the actual structure in the full-wave analysis. We then proceed to excite the system with a 5 ns pulse signal. Fig. 7 shows the comparative results of TEM and full-wave models. The non-TEM behavior can be easily identified. In particular, couplings between lines are increased significantly because of the dispersion.

We have proposed and implemented a hierarchical *bilevel waveform relaxation* algorithm for the computation of the transient response of such multiconductor systems terminated in nonlinear loads based on the model proposed here, and the computational algorithm is given in separate publications [7], [8]. An example is included here for completeness. Fig. 8(a) shows a three-conductor system terminated in CMOS inverters. The first and third lines are driven by pulse input and the middle line is connected to ground through the inverters. Fig. 8(b) plots the voltage response of the system. The logic error caused by coupling and reflection of the interconnects can be easily seen.

V. Conclusion

We have developed a computational model for a dispersive multiconductor system suitable for transient circuit analysis. Since the model is constructed based on full-wave analysis, the hybrid nature of the VLSI interconnects is taken care of, and thus the model is valid at high frequencies. Signal distortions due to the dispersive nature of a multiconductor system have been demonstrated by an example. The model is particularly suitable for the transient analysis of a multiconductor system terminated in external circuitry, especially for nonlinear terminations.

References

[1] T. Itoh and R. Mittra, "Dispersion characteristics of slot lines," *Electron. Lett.*, vol. 7, pp. 364–365, 1971.

[2] T. Itoh and R. Mittra, "Spectral-domain approach for calculating the dispersion characteristics of microstrip lines," *IEEE Trans. Microwave Theory Tech.*, vol. MTT-21, pp. 496–499, 1973.

[3] T. Itoh, Ed., *Numerical Techniques for Microwave and Millimeter-wave Passive Structures.* New York: Wiley, 1988.

[4] R. H. Jansen, "Unified user-oriented computation of shielded, covered, and open planar microwave and millimeter wave transmission-line characteristics," *IEE J. Microwaves, Opt., Acoust.*, vol. MOA-3, pp. 14–22, 1979.

[5] F. Y. Chang, "Transient analysis of lossless transmission lines in a nonhomogeneous dielectric medium," *IEEE Trans. Microwave Theory Tech.*, vol. MTT-18, pp. 616–626, Sept. 1970.

[6] E. G. Farr, C. H. Chan, and R. Mittra, "A frequency-dependence coupled-mode analysis of multiconductor microstrip lines with application to VLSI interconnection problems," *IEEE Trans. Microwave Theory Tech.*, vol. MTT-34, pp. 307–310, Feb. 1986.

[7] R. Wang and O. Wing, "Transient analysis of dispersive VLSI interconnects terminated in non-linear loads," submitted to *IEEE Trans. Computer-Aided Design.*

[8] R. Wang, "Computation of transient response of dispersive multiconductor systems," Ph.D. thesis, Columbia University, New York, NY, 1990.

[9] G. H. Golub and C. F. Vanloan, *Matrix Computations.* Baltimore: Johns Hopkins University Press, 1989.

Rui Wang received the B.S. degree from the South China Institute of Technology, Guangzhou, China, in 1982 and the M.S. and Ph.D. degrees from Columbia University, New York, NY, in 1985 and 1990, respectively.

She was a graduate research assistant at Columbia University from 1984 to 1990. She joined Advanced Micro Devices, Sunnyvale, CA, in 1990 as a Senior Design Engineer. Dr. Wang is currently a Senior Member of Technical Staff at Cadence Design Systems, Santa Clara, CA. Her research interests include VLSI interconnects, high-speed VLSI circuit design, transient analysis methods for VLSI circuits and interconnection networks, and computational microwave techniques.

Omar Wing (S'50–A'53–M'58–SM'68–F'73) received the B.S. degree from the University of Tennessee in 1950, the M.S. degree from the Massachusetts Institute of Technology in 1952, and the Eng.Sc.D. from Columbia University, New York, NY, in 1959.

Since 1959 he has been a faculty member in the Department of Electrical Engineering, Columbia University, where he is presently Professor of Electrical Engineering. He served as chairman of the Department from 1974 to 1978 and from 1983 to 1986. From 1952 he was a member of technical staff at Bell Telephone Laboratories. His current research interests include computer-aided design of high-speed electronic circuits, analysis of VLSI interconnects, modeling of heterojunction devices for circuit simulation, and optimum design of gigabit-per-second circuits for telecommunications applications.

Dr. Wing is the author or coauthor of four texts on circuit theory and a book on GaAs digital circuits. He served as President of the IEEE Circuits and Systems Society in 1976, editor of the IEEE Transactions on Circuits and Systems from 1973 to 1976, and General Chairman of the 1968 IEEE International Symposium on Circuits and Systems. He received the IEEE Centenial Medal in 1987 and the IEEE Circuits and Systems Society Award in 1989.